Desalination and Water Treatment
www.deswater.com

doi: 10.5004/dwt.2023.29904

308 (2023) 18–25
October

Evaluation of the flotation efficiency of nano and microbubbles tailored to optimize bubble size distribution using a kinetic model

Yong-Ho Choi[a], Mi-Sug-Kim[b], Yong-Hoon Jeong[a], Dong-Heui Kwak[a,*]

[a]*Department of Bio-Convergence Science, Jeonbuk National University, 9 Cheomdan-ro, Jeongeub, Jeonbuk 56212, Republic of Korea, email: kwak124@jbnu.ac.kr (D.-H. Kwak)*
[b]*School of Environmental Science, Engineering, and Policy Ph.D. Drexel University, 3141 Chestnut Street, Philadelphia, PA 19104, USA*

Received 15 March 2023; Accepted 21 August 2023

ABSTRACT

Bubble size is among the most important factors that determine flotation efficiency. The bubble used for flotation varies from nanobubbles (NBs) to microbubbles (MBs). In this study, the flotation experiments were carried out, and then the flotation efficiency was calculated based on the collision-attachment efficiency and the number of NBs and MBs bubbles using the kinetic model. The flotation efficiency was highest for tailored bubbles, followed by MBs and NBs. We determined that flotation efficiency increased as the interaction between the attachment ability of NB and the flotation ability of MB. We also determined the optimal mixing ratio by adjusting the amount of NB and MB to increase flotation efficiency. We found that the most important determinant of flotation efficiency was the ratio of MB and confirmed that NB acts as an auxiliary material that increases the attachment efficiency of floc and bubble. Also, when the amount of NB was too small flotation efficiency decreased, confirming that the flotation efficiency increased only when an appropriate ratio of NB was injected to increase the attachment efficiency.

Keywords: Bubble diameter; Dynamic light scattering; Flotation; Microbubbles; Nanobubbles

1. Introduction

Bubble size is one of the important parameters affecting flotation efficiency [1]. The flotation process can be simply described using Eq. (1).

$$E_f = E_C \times E_S \times \left(1 - E_d\right) \quad (1)$$

where E_f represents overall flotation efficiency. E_C is the collision-attachment efficiency of bubbles and particles, E_S is the efficiency at which bubble-particle aggregates (formed by the attachment of bubbles to particles) are separated from the water body, and E_d is defined as the efficiency at which bubbles and particles are detached from the formed bubble-agglomerates. Generally, E_d is close to 0 and can be ignored when conditions for flotation are well controlled.

Flotation that relies on microbubbles (MBs) is widely incorporated into traditional water treatment processes and is highly efficient at removing small particles (such as algae). The flotation process requires less coagulation time and solid–liquid separation time than a sedimentation process, so it has the advantage of configuring a small facility area and a compact process [2,3]. To date, saturator-type MBs bubble generators are mainly used in flotation systems [4]. Recently, an ejector-type bubble generator that uses cavitation has been developed. The ejector-type device generates smaller-sized bubbles [5] and enables water treatment using nanobubbles (NBs) [6]. Many researchers have

* Corresponding author.

1944-3994/1944-3986 © 2023 Desalination Publications. All rights reserved.

determined the range of bubble sizes that may be applied to water treatment systems. Although the standards developed are slightly different across each study, bubble size may roughly be divided into four categories: macro scale (>10^2), micron-scale (10^1~10^2), sub-micron scale (10^0~10^1), and nanoscale (<10^0) [7–10]. In previous studies, bubble size was measured according to pressure [11,12] and the effect of bubble size on flotation efficiency from particles was confirmed [13,14]. There are many practical limitations to measuring the size of a NB. Although one study on nano-micro size bubbles has been conducted recently [15–19], a detailed study concerning how the size of the NBs affects flotation efficiency has not been conducted to date.

The bubbles used for the actual flotation system have a wide range from nano-sized bubbles to micro-sized bubbles [20]. Flotation characteristics can be roughly classified by dividing examined bubbles in the range applied to the actual flotation process into MB and NB and excluding excessively large or small bubbles. MBs have superior solid–liquid separation efficiency bubble-particle agglomerates due to their having a higher rising rate than NBs. However, their attachment efficiency to ultra-fine floc is low due to an imbalance in hydrodynamic force [21]. NBs, in contrast, have a low hydrodynamic force during the collision-attachment phase with floc. This helps to form bubble-particle aggregates by increasing the collision attachment efficiency of bubbles and particles [22]. At actual water treatment sites, a wide range of bubbles are applied to the flotation process with a Gaussian distribution, and bubble size distribution (BSD) can vary greatly depending on the bubble generator type and the target bubble size. Therefore, combining two different sizes of bubbles can maximize the advantages of MBs and NBs to increase colliding and solid–liquid separation efficiency. Meanwhile, it has already been reported that flotation efficiency increases when NBs are included in the flotation system using MBs [23].

While bubble generators having a variety of size distributions have recently been commercialized, appropriate tailoring is required to optimize the bubbles used in actual water treatment sites. In this study, optimal flotation conditions and flotation efficiency were measured according to the optimal BSD. Thereafter, Barton et al. [24] was used to derive the constant reaction rate. By substituting this into the contact zone model developed by Haarhoff and Edzwald [25], flotation efficiency was calculated regarding the attachment efficiency (α) and the collision frequency (β). Using this information, we then developed a bubble mixing ratio that will improve flotation efficiency.

2. Materials and methods

2.1. Theoretical approach and simulation methods

Barton's kinetic theory is a model calculated as a kinetic constant or rate constant for the number of individuals considering the interaction to form an aggregate by a reversible secondary reaction between particles. Eq. (2) is the basic equation that underlies this dynamic theory:

$$n_f + n_b \xleftrightarrow{k_a, k_b} n_{\text{Agg}} \tag{2}$$

where n_f is the number of flocs, n_b is the number of bubbles, and n_{Agg} is the bubble-particle aggregates, k_a is the kinetic constant of attachment, and k_b is the kinetic constant of breakage. Eq. (3) expresses this as a secondary reaction:

$$\frac{dn_f}{dt} = -k_a n_f n_b + k_b n_{\text{agg}} \tag{3}$$

where k_a is the same as $\alpha_{\text{fb}}\beta_{\text{fb}}$ and n_{agg} is the number of removed particles as expressed by Eq. (4).

$$\frac{dn_f}{dt} = -\alpha_{\text{fb}}\beta_{\text{fb}} n_f n_b + k_b\left(n_{f0} - n_f\right) \tag{4}$$

where α_{fb}, β_{fb}, is the attachment efficiency and the collision frequency, and n_{f0} is the number of raw flocs. Eqs. (5) and (6) can be obtained by expressing Eq. (4) as a first-order reaction equation for n_f and substituting it into the distribution coefficient (γ_t) indicating the floc distribution concentration between the bubble and floc.

$$n_f = n_{f_0} e^{-(\alpha\beta n_b + k_b)t} + \frac{k_b n_{f_0}}{\left(\alpha\beta n_b + k_b\right)}\left(1 - e^{-(\alpha\beta n_b + k_b)t}\right) \tag{5}$$

$$\gamma_t = \frac{n_{f_0} R}{n_f C_b} = \frac{\dfrac{n_{f_0}\left(n_{f_0} - n_f\right)}{n_f}}{n_f C_b} = \frac{\dfrac{\left(n_{f_0} - n_f\right)}{C_b}}{n_f}$$
$$= \frac{1}{c_b}\left(\frac{1}{e^{-(\alpha\beta n_b + k_b)t} + \dfrac{k_b}{\alpha\beta n_b + k_b}\left(1 - e^{-(\alpha\beta n_b + k_b)t}\right)} - 1\right) \tag{6}$$

where C_b is the mass concentration of bubbles, t is the reaction time, and R is the flotation efficiency. In Eq. (6), floc and bubble once attached can be expressed as k_b = 0 under the assumption that desorption does not occur. Once again, Eq. (6) can be expressed as Eqs. (7) and (8), and finally the equation of $k = \alpha_{\text{ab}}\beta_{\text{ab}}n_b$ is obtained, in which where k is the constant reaction rate of the first-order reaction.

$$\gamma_t C_b = \left(\frac{1}{e^{-(\alpha\beta n_b)t}} - 1\right) \rightarrow \ln\left(\gamma_t C_b + 1\right) = -\alpha_{\text{fb}}\beta_{\text{fb}} n_b t \approx -kt \tag{7}$$

$$\gamma_t C_b + 1 = \frac{n_{f_0}}{n_f} \rightarrow \ln\left(\frac{n_{f_0}}{n_f}\right) = \ln\left(\gamma_t C_b + 1\right)$$
$$= -\alpha_{\text{fb}}\beta_{\text{fb}} n_b t \approx -kt \rightarrow \ln\left(\frac{n_f}{n_{f_0}}\right) = -kt \tag{8}$$

where α and β can be calculated by substituting the equations calculated using the kinetic theory into the white-water blanket filtration type models (WWBFM), which are the contact area models of flotation separation. The WWBFM model of Haarhoff and Edzwald [25] uses the concept of a single simple collector collision efficiency, and hydrodynamic interactions and interparticle effects are not considered.

To facilitate expression in the model, number concentration (n_b) and volume concentration ($\varnothing_b$) are expressed in Eqs. (9) and (10). The basic formula of the model is Eq. (11). When single collector collision efficiency (η_T) is used to explain particle movement, k_a can be expressed as Eq. (12).

$$n_b = \left(\frac{C_b}{\rho_b}\right)\left(\frac{6}{\pi d_b^3}\right) \tag{9}$$

$$\varnothing_b = \left(\frac{C_b}{\rho_b}\right) \tag{10}$$

$$\frac{dn_f}{dt} = -k_a n_f n_b \tag{11}$$

$$k_a = \alpha_{fb}\eta_T v_b A_b n_b \tag{12}$$

where ρ_b is the bubble density and d_b is the bubble diameter. The projected area of the bubble (A_b) is replaced by ($\pi d_b^2/4$). Eq. (13) is obtained by replacing n_b with $\varnothing_b$ using Eqs. (9) and (10). If this is again expressed as a first-order reaction equation of n_f with respect to the contact time (t_{cz}), it can be expressed as Eq. (14).

$$\frac{dn_f}{dt} = -\frac{3}{2}\left(\frac{\alpha_{fb}\eta_T v_b \Phi_b}{d_b}\right) \tag{13}$$

$$\frac{n_f}{n_{f_0}} = \left[\exp\left(-\frac{3}{2}\left(\frac{\alpha_{fb}\eta_T v_b \Phi_b}{d_b}\right)t_{cz}\right)\right] \tag{14}$$

Finally, substituting into the kinetic theory, Eq. (12) is expressed as $\eta_T v_b A_b n_b = \beta_{fb}$, and finally expressed as Eq. (15).

$$k = \frac{3}{2}\left(\frac{\alpha_{fb}\eta_T v_b \Phi_b}{d_b}\right) = \alpha_{fb}\beta_{fb}n_b \tag{15}$$

The flotation efficiency is affected by the bubble size, which affects α, β, and n_b. In this study, the effect of each of these three factors on flotation efficiency was calculated using the contact model and the dynamic theory and evaluated by comparing it with the actual flotation efficiency. We were then able to predict the optimal mixing ratio of bubbles through the calculated model and confirm that a proper mix of NB and MB improves flotation efficiency.

2.2. Bubble size measurements

As shown in Fig. 1, the produced MB was injected into the flotation column as the pressure of the pressurizing device. 5 atm pressured bubble diameter was calculated according to microscope charged coupled CCD camera (INFINITY 2-2C, Teledyne Lumenera, Canada). To measure the most accurate size distribution, the focus of the camera lens was placed in the center of the column, and after the bubbles were injected, the shooting started in the area where the bubble cloud was created. After taking a video, it was divided into 1 frame units. The size of each bubble size was measured with an image capture module by lowering the exposure and shooting as clearly as possible. It was measured repeatedly and presented as an average value.

NB size distribution was measured using dynamic light scattering (DLS). The measurement was carried out through a stabilization process in which the NB generator was operated for a sufficient period to obtain the most consistent value. 1 mL of the sample collected from the experimental column was then sprayed with NB according to the analysis capacity and analyzed with dynamic light scattering using a Zen 3600, Malvern Instruments (UK). To reduce the experimental error and obtain a reliable value, this analysis was repeated, this time calculated by arithmetic mean.

Nanobubbles require more precise measurements than microbubbles. There are several ways to measure the size of an NB. Either a laser particle-size analyzer (LPSA), which measures particle size using laser dispersion, scattering,

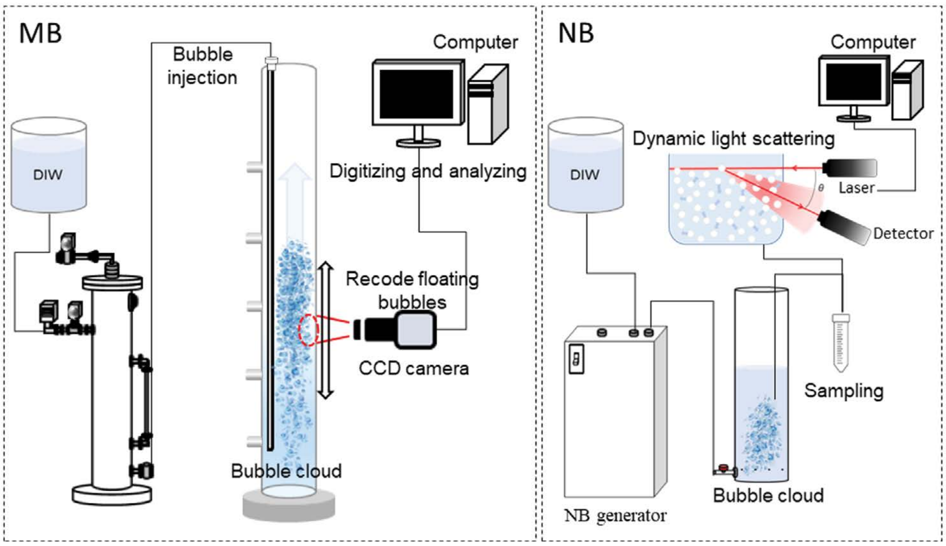

Fig. 1. Schematic diagram of apparatuses for measuring MB and NB size using charge-coupled device (CCD) camera and dynamic light scattering.

and refraction, nanoparticle tracking analysis (NTA), which tracks the movement of nanoparticles by Brownian motion, or electrophoresis analytical equipment can be used. DLS is an instrument generally used to measure the size distribution of nano ~ sub-micron particles, and some researchers have used it to measure the size of NBs [26–28]. In DLS, laser light scattered at various intensities according to the Brownian motion of sample particles is analyzed through photon intensity and autocorrelation function.

2.3. Experimental condition

An artificial sample was prepared by mixing kaolin particles with distilled water. Kaolin particles are widely used in water treatment experiments. For the calculation of the flotation rate (*R*, %) for the change of conditions, the representative value (average) was determined by measuring turbidity (2100P, Hach, USA) of ten or more samples before and after the flotation experiments. Using this data, the flotation efficiency was calculated.

To examine the flotation efficiency of MBs and NBs, a laboratory-scale batch-type flotation separation test apparatus was fabricated (Fig. 2). The volume of the air dissolving tank (saturator) was approximately 0.67 L, and it was made of stainless steel to take advantage of its high operating pressure. For the flotation separation experiment, the Jar test was performed on an artificial sample prepared in advance to determine the optimal coagulant injection rate. A series of flotation experiments were then performed. The size of the flotation column was 1.5 L (10 cm in diameter, 17 cm in height). This was filled with 0.5 L of the artificial sample prepared in advance, as well as poly aluminum chloride (PAC, $[Al(OH)m{\cdot}Cl_6\text{-}m]n$) in the coagulant. To aggregate the particles 30 ppm of PAC was injected, followed by rapid stirring at about 125 rpm for 1 min, further followed by slow stirring at 40 rpm for 5 min. In some cases, sodium hydroxide (NaOH) was used as an alkali agent to supplement the alkalinity required for agglomeration.

Saturated water was injected according to the injection amount. To observe the floating of the particles, bubbles were sprayed under three conditions: NB, MB, and mixed bubbles. When injecting mixed bubbles, nanobubbles were injected first and then microbubbles were sequentially injected in order to clearly grasp the effect of nanobubbles. In the operation, saturated water (milky water) was sprayed in a saturator pressurized to the previously prepared flotation column sample until the recycle ratio reached about 20%. Saturated water was injected in a turbulent state to increase the number of collisions between bubbles and particles. After a sufficient contact time, flotation was maintained for about 5 min, and the experiment was conducted. Once the flotation finished, after removing the scum floating on the surface layer, clean subnatant was collected from the bottom of the column and analyzed. Thereafter, the floating efficiency of the model and the experimental data was compared by adjusting the NB/MB ratio.

3. Results and discussion

3.1. Bubble size distribution

Bubble size is an important factor affecting flotation efficiency. Information regarding bubble size is required to

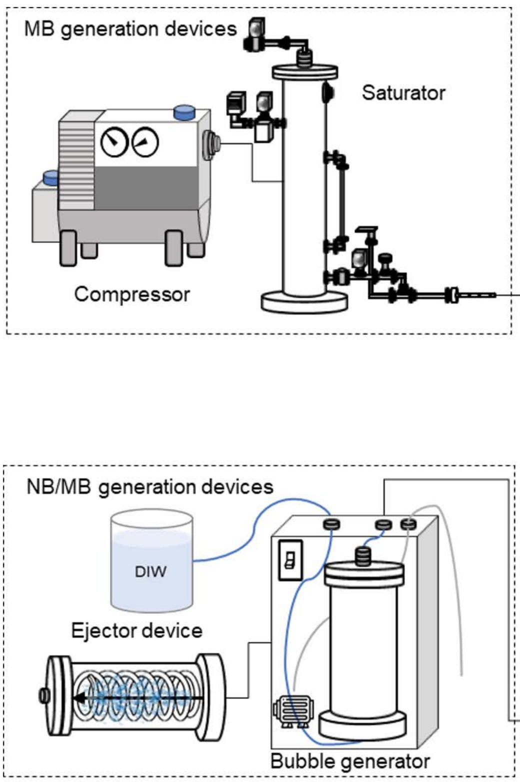

Fig. 2. Schematic diagram of lab scale flotation device for particle separation.

accurately assess flotation efficiency. In this study, the bubble size was measured using a CCD camera to find out how the bubble size affects the flotation efficiency. The size of MBs calculated from repeated measurements ranged from 23.61 to 83.94 μm at 5 bar. In general, NBs can also occur in MB generators, but the amount is negligible. However, it should be considered that the amount of NB generation may increase depending on the type of MB generator and operating conditions in the field.

In contrast, in the case of NB, the floating velocity equation cannot be used to determine the size of the NBs because it cannot confirmed by the naked eye. NB size measurement was performed using DLS. The distribution of NBs measured through DLS is shown in Fig. 3. The bubbles ranged in size from 350 to 530 nm, with bubbles of an average size of 460 nm making up the greatest proportion. Tables 1 and 2 show the MB size range and average size at each atmospheric pressure, as well as the specifications associated with the nanobubble generator. Using these results above, we determined the optimal flotation efficiency for each bubble size in the flotation experiment.

3.2. Collision-attachment efficiency

Model results were derived by substituting the data obtained from the flotation experiment into WWBFM. In flotation, α and β acting between bubbles and floc play a large role in the formation of bubble-particle aggregates [22], and in turn have a significant influence on the flotation efficiency. In the single bubble simulation, α showed a higher value as the size of the bubble increased, and gradually decreased as the size of the bubble increased. β showed the lowest value when the size of the bubble was small, and gradually increased as the size of the bubble increased. It is known from the literature that the smaller the bubble size, the higher the contact efficiency but the lower the collision [21,22]. Conversely, it was confirmed that as the bubble size increased, the contact efficiency decreased, but the collision frequency increased. Fig. 4 is αβ compare graph, which changes according to the bubble size, with n_b. n_b can be calculated using Eq. (9) and the value obtained by calculating the dynamics theory and the size of the bubble through experiments, as well as the volume concentration of the bubble. Looking at the obtained changes in factors, we observed that αβ gradually increased along with the bubble size. n_b was seen to decrease as the bubble size increases. This means that the smaller the bubble size, the smaller the collision-attachment efficiency and the greater the number of bubbles. As the size of the bubbles increase, the collision-attachment efficiency increases, and the number of bubbles drops.

Flotation efficiency can therefore be determined by reference to these three functions: n_b, α, and β. It is used to interpret and evaluate the results obtained in the flotation

Table 1
Size distribution of microbubbles

Pressure of saturator (bar)	Bubble size range (average) (μm)
5.0	25.61 ~ 83.94 (53.18)

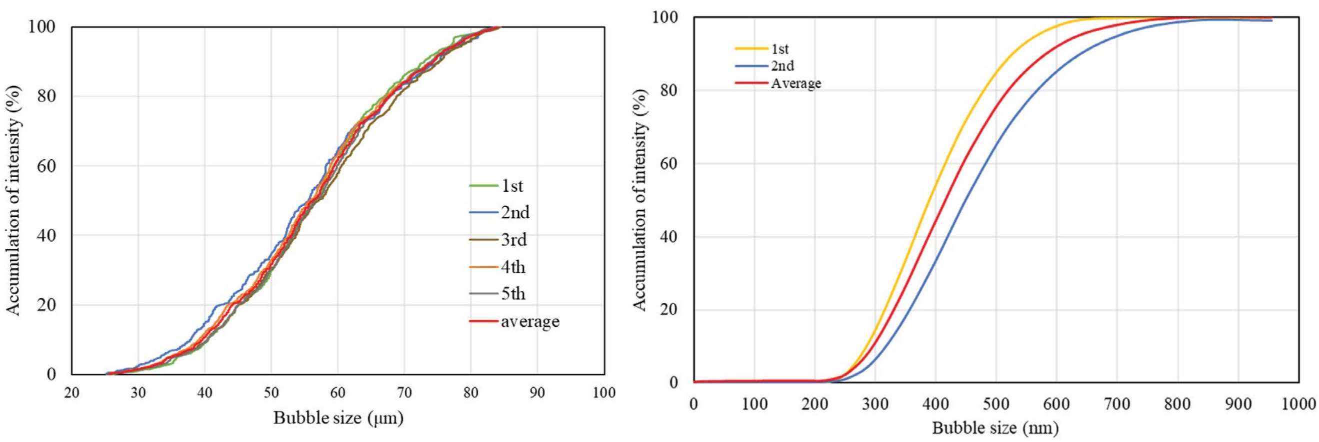

Fig. 3. Bubble size distribution NB and MB, (a) measured and calculated values of MBs using rising velocity equation, (b) average of NB measurement using dynamic light scattering.

Table 2
Specification associated with nanobubble generator and average bubble size

Pump	Mixing chamber	Bubble
Flow rate: 0.45 L/min	Material: stainless	Average bubble size: 459 nm
Head: 2.0 m	Shape: cylinder	Bubble volume concentration: 0.08513 mL/mL
Motor power: 100 W	Volume: 1.4 L	
Air flow rate 30 mL/min	Height: 180 mm	
	Diameter: 100 mm	

experiment. To evaluate the flotation efficiency of NBs and MBs, we examined how each of these functions works according to the bubble size based on the results obtained from the experiment.

3.3. Flotation efficiency

The flotation experiment was carried out by first dividing bubbles by size (NB and MB). Based on the calculated model results, we assumed that better flotation efficiency would be obtained if the experiment was conducted utilizing the strengths of NB and MB. The flotation efficiency was then analyzed and evaluated using the results of the modeling. The experimental values for flotation are shown in Fig. 5.

NB bubbles had the lowest flotation efficiency, with NB+MB bubbles showing the highest efficiency. This is like the results obtained in the literature introducing previously conducted studies showing better efficiency than microbubbles when mixing nanobubbles and microbubbles [29].

This can be interpreted as a function of n_b, α, and β as calculated through the previously discussed model. NB has many bubbles, but the collision-attachment efficiency between bubbles and flocks is small, so the flotation efficiency is low. MB, in contrast, has a large collision-attachment efficiency, but the number of bubbles is significantly lower. Here, it can be seen that no matter how large the number of bubbles is, if the collision-attachment efficiency between the bubbles and floc is lowered, the flotation efficiency will eventually decrease. Finally, we hypothesize that the highest efficiency was shown when NB and MB bubbles were mixed is because the high number of bubbles in NB and the high collision-attachment efficiency of MB complement each other to improve this quality. NB and MB have a mutually reinforcing positive effect on each other's flotation, and mixing the NB and MB may significantly improve flotation efficiency.

The flotation separation test in this experiment was conducted in stationary conditions in the flotation column. In the flotation system in the field, however, influents with flocs and bubbles could flow into turbulence through the existing bubble layer. Therefore, the attachment efficiency and collision frequency need to be modified properly for application to the flotation process in the field.

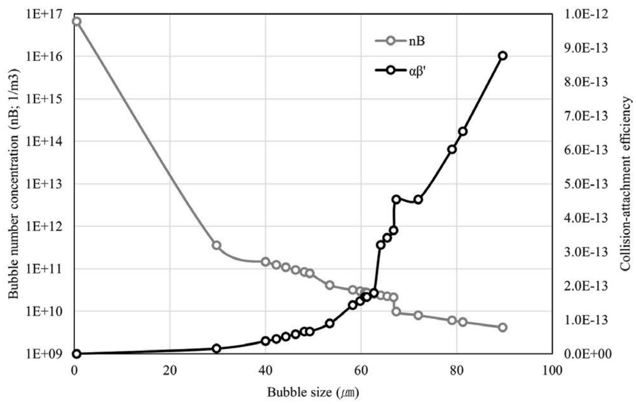

Fig. 4. Variation of αβ and n_b in terms of bubble size.

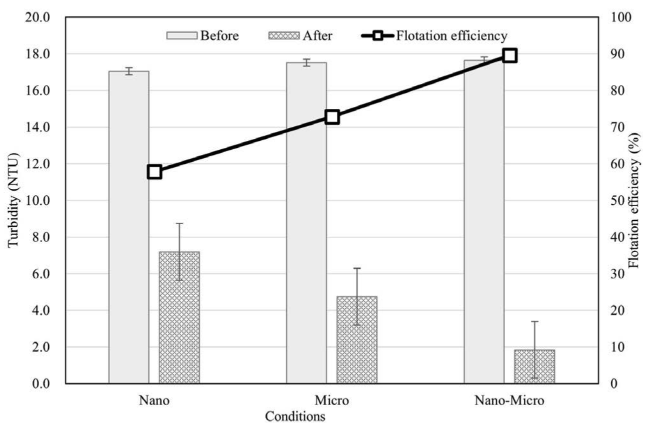

Fig. 5. Variation of flotation efficiency depending on NB and MB.

3.4. Tailoring NB/MB ratio to improve flotation efficiency

The flotation experiment confirmed that the mixing of NB and MB had a significant effect on flotation efficiency. Therefore, the optimal mixing ratio between NB and MB needed to be determined. The numerical fraction of the NB to MB ratio (F) can be defined as Eq. (16).

$$F = \frac{n_{\mathrm{nb}}}{n_{\mathrm{mb}}} \tag{16}$$

where n_{nb} is the number of nano-bubbles and n_{nb} is the number of microbubbles.

After the calculated bubble ratio, then compared the predicted results with the experimental results. In order to obtain a high level of flotation, the optimal mixing ratio had to be determined. The flotation efficiency of the mixed bubbles was predicted based on the values of n_b, α, and β which were calculated through the kinetic theory. However, that flotation efficiency may differ depending on the properties of the target particles, and that the mixing ratio can be applied differently depending on the test target. When the distribution of bubbles was compared while adjusting the ratio of NB and MB, Fig. 6 is a graph expressing the distribution according to the bubble size shown while adjusting the ratio of NB and MB. And the predicted and experimental results using the model are shown in Fig. 7. It shows that the measured NB and MB distributions vary with the NB and MB ratios.

In the model, the higher the NB ratio, the lower the flotation efficiency, and the higher the MB ratio the higher the flotation efficiency. The experimental results in contrast, showed somewhat different results from these. The highest flotation efficiency among the bubble mixtures tested experimentally was observed when the ratio of NB to MB was 3:7. As the ratio of MB increased, or more NB was injected than MB, the flotation efficiency gradually decreased. When mix and inject NB and MB, the flotation efficiency increased along with the amount of injected MB.

The model and experimental results differed because too little NB, which acts during the collision-attachment process with the actual floc, was injected, so the bubbles may not have been mixed well. We hypothesize that the anticipated

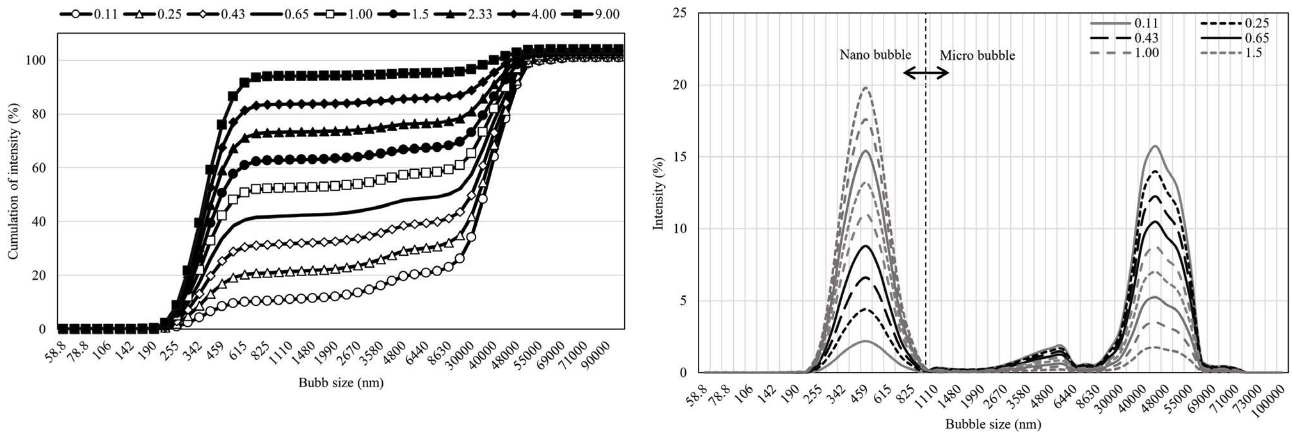

Fig. 6. (a) Cumulation bubble size distribution in terms of NB/MB blending ratio and (b) size distribution of the bubble depends on the MB/NB ratio.

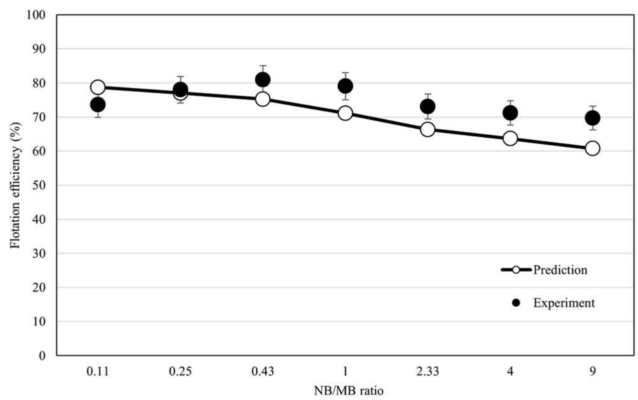

Fig. 7. Comparison of predicted and experimental flotation efficiency.

effect of NB, that is, increasing the attachment efficiency between floc and bubbles, is thus not properly brought about. Through comparison, we confirmed that MB had a significant effect on flotation efficiency in the mixed MB & NB bubbles, but that flotation efficiency was improved only when NB was injected at an appropriate ratio or more. We also confirmed that NB can compensate for the low attachment efficiency of MB, if there is no MB even if the number of cells in NB is large and the attachment efficiency of single cells is high, the efficiency does not increase. Through these prediction results, it was confirmed that bubble mixing is another way to improve the flotation efficiency.

4. Conclusion

We evaluated the collision and attachment characteristics of NBs and MBs, and variations in the number of bubbles under the various collision-attachment efficiency between bubbles and floc for bubbles of various sizes using a model. Based on the simulation results of the collision-attachment efficiency, the terminal flotation efficiency was calculated in the various size ranges of bubbles. We then predicted the optimal bubble mixing conditions and compared this prediction with experimental results.

As the average bubble size increases, collision frequency increases and the attachment efficiency decreases. Overall flotation efficiency is affected differently depending on the functions of n_b, α, and β, with NBs having a high n_b, but flotation efficiency remained low due to a low levitation force. MB, in contrast, has a low n_b but a higher flotation efficiency than NB due to its high levitation force.

Our experiment revealed that flotation efficiency was assessed as follows: NB (58%) < MB (73%) < NB+MB (90%). This is attributable to the high attachment efficiency of the NB and the high levitation force of the MB. As a result of the prediction in the model, if the bubbles are mixed and used, NB and MB complement the weak parts and can improve the flotation efficiency.

When the amount of MB was higher than that of NB in the bubble mixture, efficiency improved. However, as we compared the experimental results with the model results, we confirmed that in the event that MB were excessively injected, efficiency would decrease, and that flotation efficiency can be increased only by proper mixing with a certain amount of NBs injected.

Acknowledgements

This work was funded by the National Research Foundation of Korea (NRF: NRF-2019R1A2C1006441) with a grant from the Ministry of Environment.

References

[1] J.-C. Tsai, M. Kumar, S.-Y. Chen, J.-G. Lin, Nano-bubble flotation technology with coagulation process for the cost-effective treatment of chemical mechanical polishing wastewater, Sep. Purif. Technol., 58 (2007) 61–67.
[2] M. Takahashi, Base and technological application of microbubble and nanobubble, Mater. Integr., 22 (2009) 2–19.
[3] A. Azevedo, R. Etchepare, J. Rubio, Raw water clarification by flotation with microbubbles and nanobubbles generated with a multiphase pump, Water Sci. Technol., 75 (2017) 2342–2349.
[4] V.R. Fanaie, M. Khiadani, G. Sun, Effect of salinity and temperature on air dissolution in an unpacked air saturator of a dissolved air flotation system, Desal. Water Treat., 170 (2019) 91–100.

[5] H.-S. Kim, J.-Y. Lim, S.-Y. Park, J.-H. Kim, Effects of distance of breaker disk on performance of ejector type microbubble generator, KSCE J. Civ. Eng., 22 (2018) 1096–1100.
[6] K. Ulatowski, P. Sobieszuk, Gas nanobubble dispersions as the important agent in environmental processes–generation methods review, Water Environ. J., 34 (2020) 772–790.
[7] A. Agarwal, W.J. Ng, Y. Liu, Principle and applications of microbubble and nanobubble technology for water treatment, Chemosphere, 84 (2011) 1175–1180.
[8] D. Kobayashi, Y. Hayashida, K. Sano, K. Terasaka, Agglomeration and rapid ascent of microbubbles by ultrasonic irradiation, Ultrason. Sonochem., 18 (2011) 1193–1196.
[9] R. Pérez-Garibay, E. Martínez-Ramos, J. Rubio, Gas dispersion measurements in microbubble flotation systems, Miner. Eng., 26 (2012) 34–40.
[10] V. Ross, A. Singh, K. Pillay, Improved flotation of PGM tailings with a high-shear hydrodynamic cavitation device, Miner. Eng., 137 (2019) 133–139.
[11] S. Burns, S. Yiacoumi, C. Tsouris, Microbubble generation for environmental and industrial separations, Sep. Purif. Technol., 11 (1997) 221–232.
[12] W.-H. Zhang, J. Zhang, B. Zhao, P. Zhu, Microbubble size distribution measurement in a DAF system, Ind. Eng. Chem. Res., 54 (2015) 5179–5183.
[13] N. Ahmed, G. Jameson, The effect of bubble size on the rate of flotation of fine particles, Int. J. Miner. Process., 14 (1985) 195–215.
[14] G. Collins, G. Jameson, Experiments on the flotation of fine particles: the influence of particle size and charge, Chem. Eng. Sci., 31 (1976) 985–991.
[15] M. Alheshibri, A. Al Baroot, L. Shui, M. Zhang, Nanobubbles and nanoparticles, Curr. Opin. Colloid Interface Sci., 55 (2021) 101470, doi: 10.1016/j.cocis.2021.101470.
[16] M.-S. Kim, D.-H. Kwak, Comparative evaluation of particle separation efficiency based on carbon dioxide and air bubble sizes in flotation separation processes, Sep. Purif. Technol., 138 (2014) 161–168.
[17] D.-H. Kwak, S.-J. Kim, H.-K. Lee, H.-J. Jung, J.-W. Lee, P.-G. Chung, Hydrodynamic collision efficiency and flotation characteristics of inorganic particles in DAF process, J. Korean Soc. Water Wastewater, 16 (2002) 655–662.
[18] M.-S. Kim, M. Han, T.-I. Kim, J.-W. Lee, D.-H. Kwak, Effect of nanobubbles for improvement of water quality in freshwater: flotation model simulation, Sep. Purif. Technol., 241 (2020) 116731, doi: 10.1016/j.seppur.2020.116731.
[19] E.-J. Lee, Y.-H. Kim, H.-S. Kim, A. Jang, Influence of microbubble in physical cleaning of MF membrane process for wastewater reuse, Environ. Sci. Pollut. Res., 22 (2015) 8451–8459.
[20] R. Etchepare, A. Azevedo, S. Calgaroto, J. Rubio, Removal of ferric hydroxide by flotation with micro and nanobubbles, Sep. Purif. Technol., 184 (2017) 347–353.
[21] Z. Dai, D. Fornasiero, J. Ralston, Particle–bubble collision models—a review, Adv. Colloid Interface Sci., 85 (2000) 231–256.
[22] D. Tao, A. Sobhy, Nanobubble effects on hydrodynamic interactions between particles and bubbles, Powder Technol., 346 (2019) 385–395.
[23] R. Ahmadi, D.A. Khodadadi, M. Abdollahy, M. Fan, Nano-microbubble flotation of fine and ultrafine chalcopyrite particles, Int. J. Min. Sci. Technol., 24 (2014) 559–566.
[24] L.E. Barton, M. Therezien, M. Auffan, J.-Y. Bottero, M.R. Wiesner, Theory and methodology for determining nanoparticle affinity for heteroaggregation in environmental matrices using batch measurements, Environ. Eng. Sci., 31 (2014) 421–427.
[25] J. Haarhoff, J.K. Edzwald, Dissolved air flotation modelling: insights and shortcomings, J. Water Supply Res. Technol. AQUA, 53 (2004) 127–150.
[26] S. Nazari, A. Hassanzadeh, Y. He, H. Khoshdast, P.B. Kowalczuk, Recent developments in generation, detection and application of nanobubbles in flotation, Minerals, 12 (2022) 462, doi: 10.3390/min12040462.
[27] X. Ma, M. Li, X. Xu, C. Sun, On the role of surface charge and surface tension tuned by surfactant in stabilizing bulk nanobubbles, Appl. Surf. Sci., 608 (2023) 155232, doi: 10.1016/j.apsusc.2022.155232.
[28] W. Xu, Y. Wang, Q. Huang, X. Wang, L. Zhou, X. Wang, B. Wen, N. Guan, J. Hu, X. Zhou, The generation and stability of bulk nanobubbles by compression-decompression method: the role of dissolved gas, Colloids Surf., A, 657 (2023) 130488, doi: 10.1016/j.colsurfa.2022.130488.
[29] W. Shen, D. Mukherjee, N. Koirala, G. Hu, K. Lee, M. Zhao, J. Li, Microbubble and nanobubble-based gas flotation for oily wastewater treatment: a review, Environ. Rev., 30 (2022) 359–379.